Sogang University
SMOS Laboratory

Weekly Meeting
Journal Club

Molecular conformation of DPPC phospholipid Langmuir and Langmuir–Blodgett monolayers studied by heterodyne-detected vibrational sum frequency generation spectroscopy

Naoki Takeshita , Masanari Okuno and Taka-aki Ishibashi

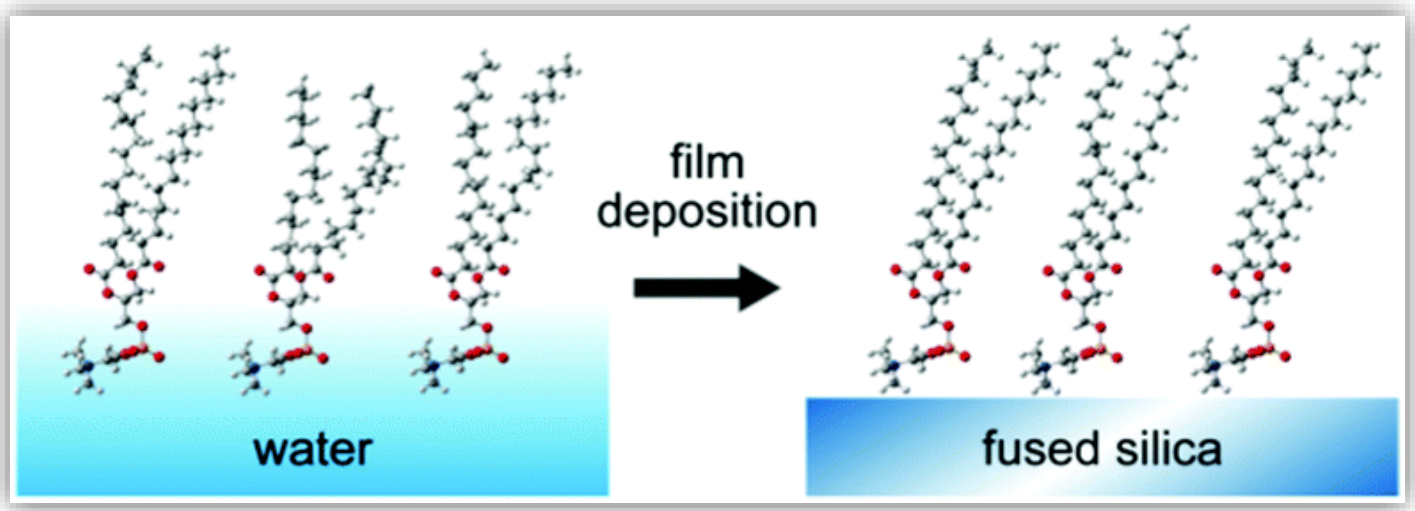

K. Sona
27-May-2017

Introduction

Langmuir Monolayer And Langmuir-Blodgett monolayer

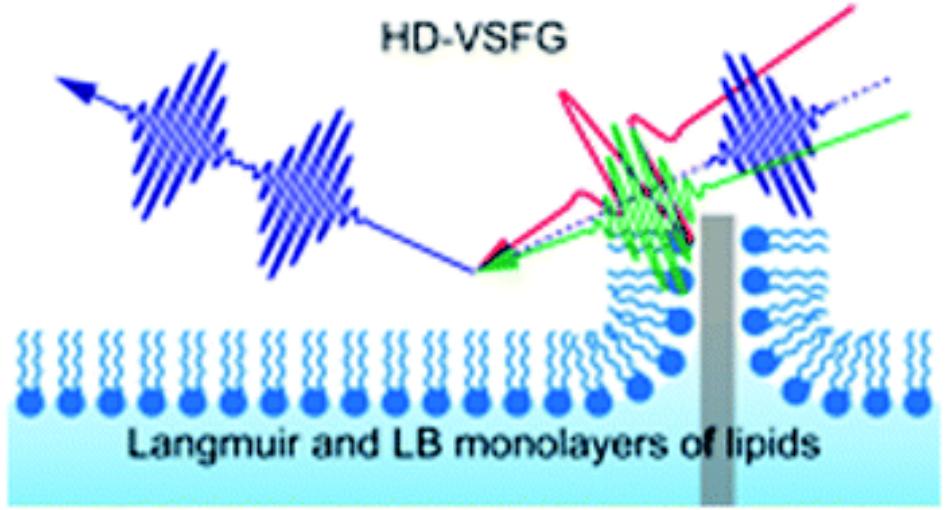

Important applications include fundamental studies of biological membranes: L and LB as models to address the intermolecular interactions between membrane molecules and bioactive molecules.

Membrane insertion processes of

- Protein
- Peptides
- Surfactants.

Use HD-VSFG spectra
(CH stretching region)
To Examine the conformations

L monolayer on water
(with various surface pressure)

LB on fused silica
(with various surface pressure)

What they found

The molecular conformations and orientations on LB monolayers were slightly but appreciably different from corresponding Langmuir monolayers.

Weak VSFG bands at 2850 and 2935 cm^{-1}, which have not been perceived so far, will be also reported

Experimental [Sample Preparation]

DPPC

Langmuir Monolayer

Surface pressure

3, 6, 9, 24, 45 mN m^{-1}

65mm

65mm Teflon trough

To form Langmuir Monolayer: DPPC solution 1mg mL^{-1}

To form Langmuir Blodgett Monolayer:
Fused silica substrate was vertically dipped at 20mm min^{-1}

75mm

Langmuir-Blodgett Monolayer

Surface pressure

1, 6, 9, 20, 40 mN m^{-1}

364 mm KSV Minitrough 2000

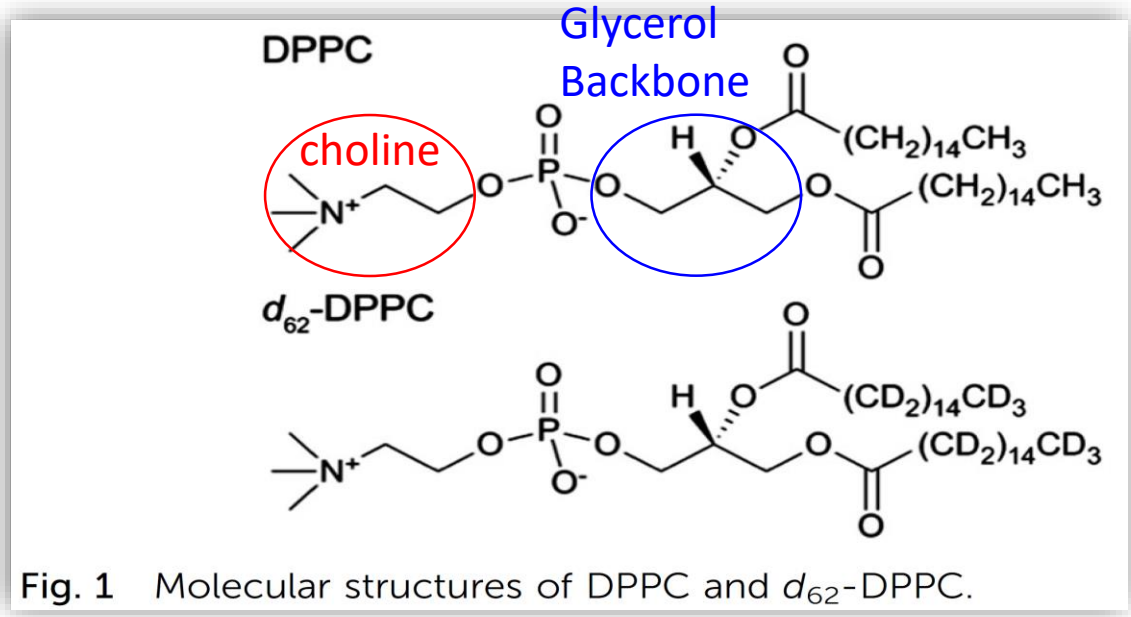

Fig. 1 Molecular structures of DPPC and d_{62}-DPPC.

To identify the vibrational modes of the methyls and methylenes in the head group, Langmuir and LB monolayers of **deuterated DPPC** were also measured.

8 , 17, 35 mN m^{-1}

Experimental [HD-VSFG measurement]

Ti:sapphire Laser
800 nm, 100 fs
3.5 mJ, 1kHz

$\frac{2}{3} \times 3.5$ mJ Narrow-band Second-harmonic generator
(SHBC, coherent)
400 nm (5ps, 8cm^{-1})

Optical parametric amplifier,
TOPAS-400-fs-WL, Coherent
visible 630nm, bandwidth 10 cm^{-1}

$\frac{1}{3} \times 3.5$ mJ Optical parametric amplifier,
TOPAS-800-fs, Coherent
IR 3400nm (2900 cm^{-1}) , fwhm 200 cm^{-1}

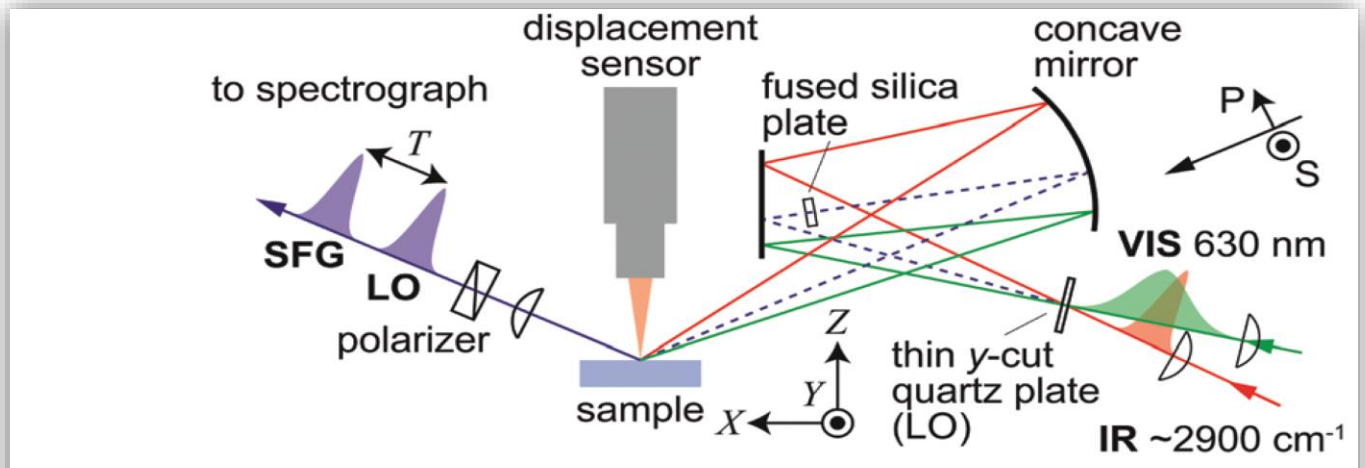

Fig. 2 Schematics of HD-VSFG setup.

- y-cut quartz plate 10μm
- Retardation 2.5 ps
- IR angle 63°
- Visible angle 72°

Results and discussion [π-A isotherm of DPPC monolayers]

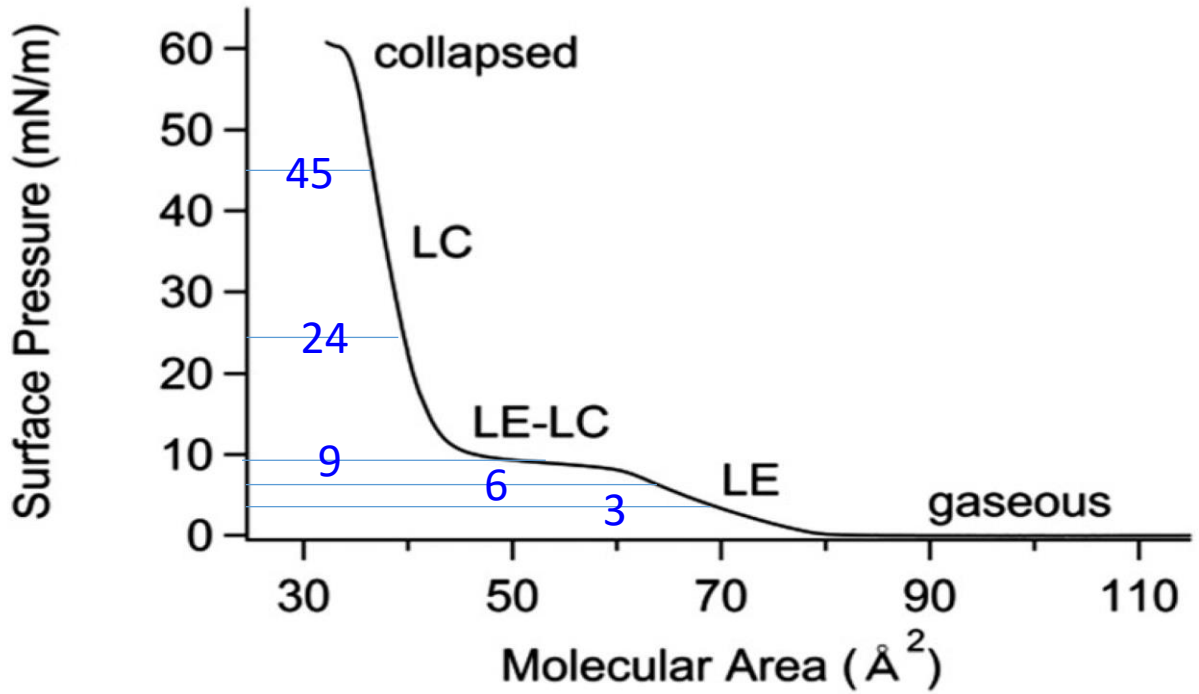

Fig. 3 π–A isotherm of DPPC on water at room temperature (25 °C)

Results and discussion [Im[$\chi^{(2)}$] spectra of DPPC monolayers]

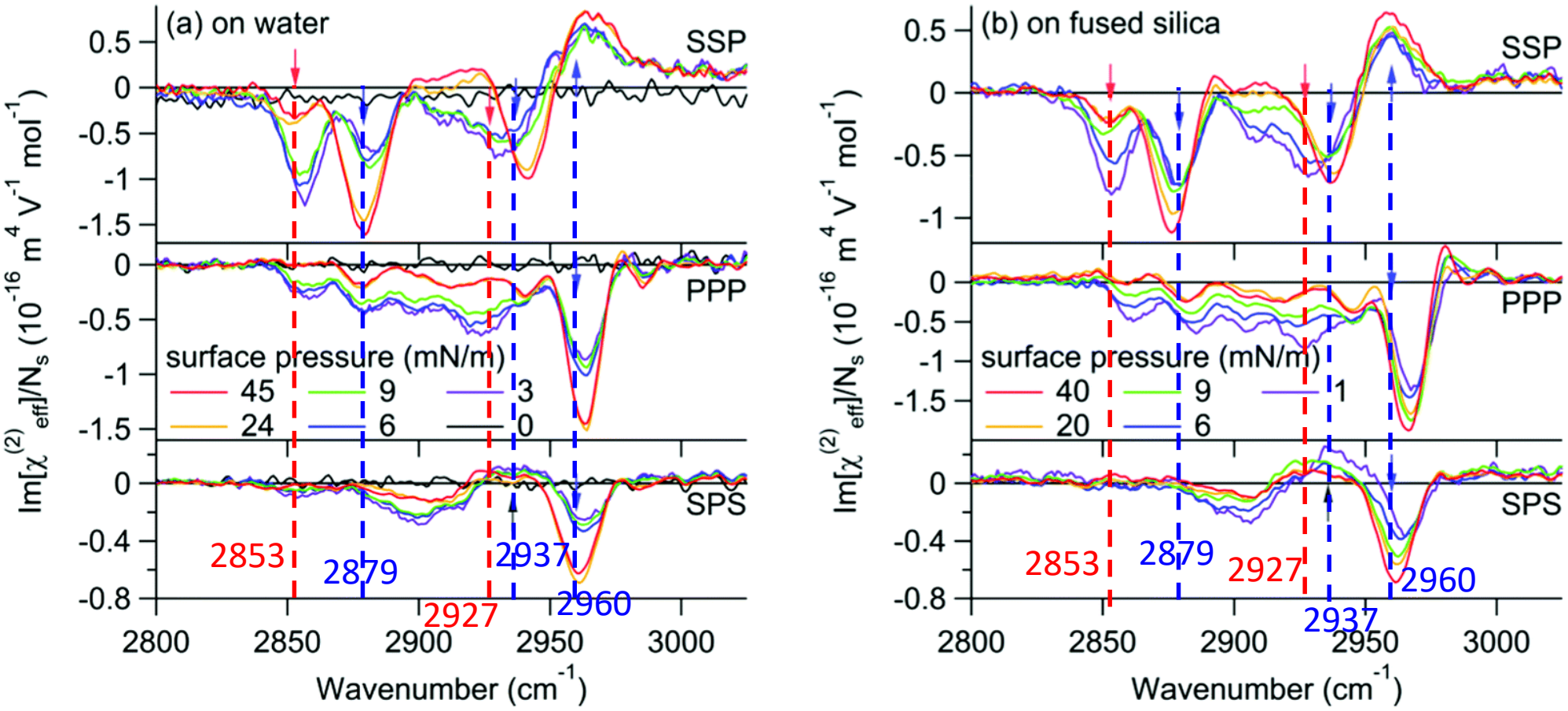

2853	2879	2927	2937	2960
CH_2 ss	CH_3 ss	CH_2 FR	CH_3 FR	CH_3 as

Fig. 4 Im[$\chi^{(2)}$] spectra of DPPC in the CH stretching region in the SSP, PPP, and SPS polarization combinations. (a) Langmuir monolayers on water at various surface pressures and (b) LB monolayers on fused silica substrates deposited at various surface pressures. All spectra correspond to the susceptibility per one mole of lipid molecules. The red arrows denote the vibrational bands attributed to methylene groups and the blue ones denote those attributed to methyl groups in the alkyl chains of DPPC. The positions of these arrows correspond to those determined by the fitting analyses of $\chi^{(2)}_{eff,SSP}$ spectra. The gray arrows denote the band we first identified in this study. See text for more details.

Results and discussion [π-A isotherm of d_{62}-DPPC Langmuir and LB monolayers]

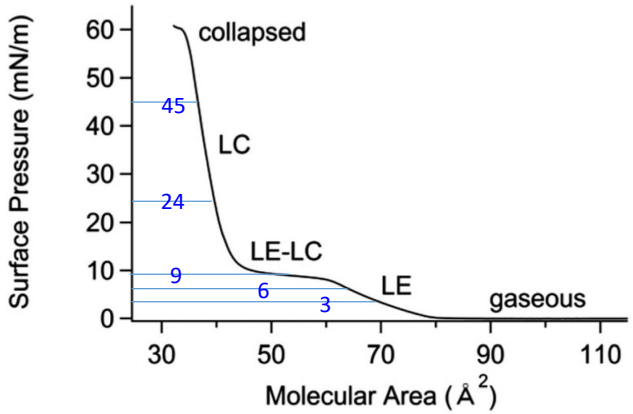

Fig. 3 π–A isotherm of DPPC on water at room temperature (25 °C)

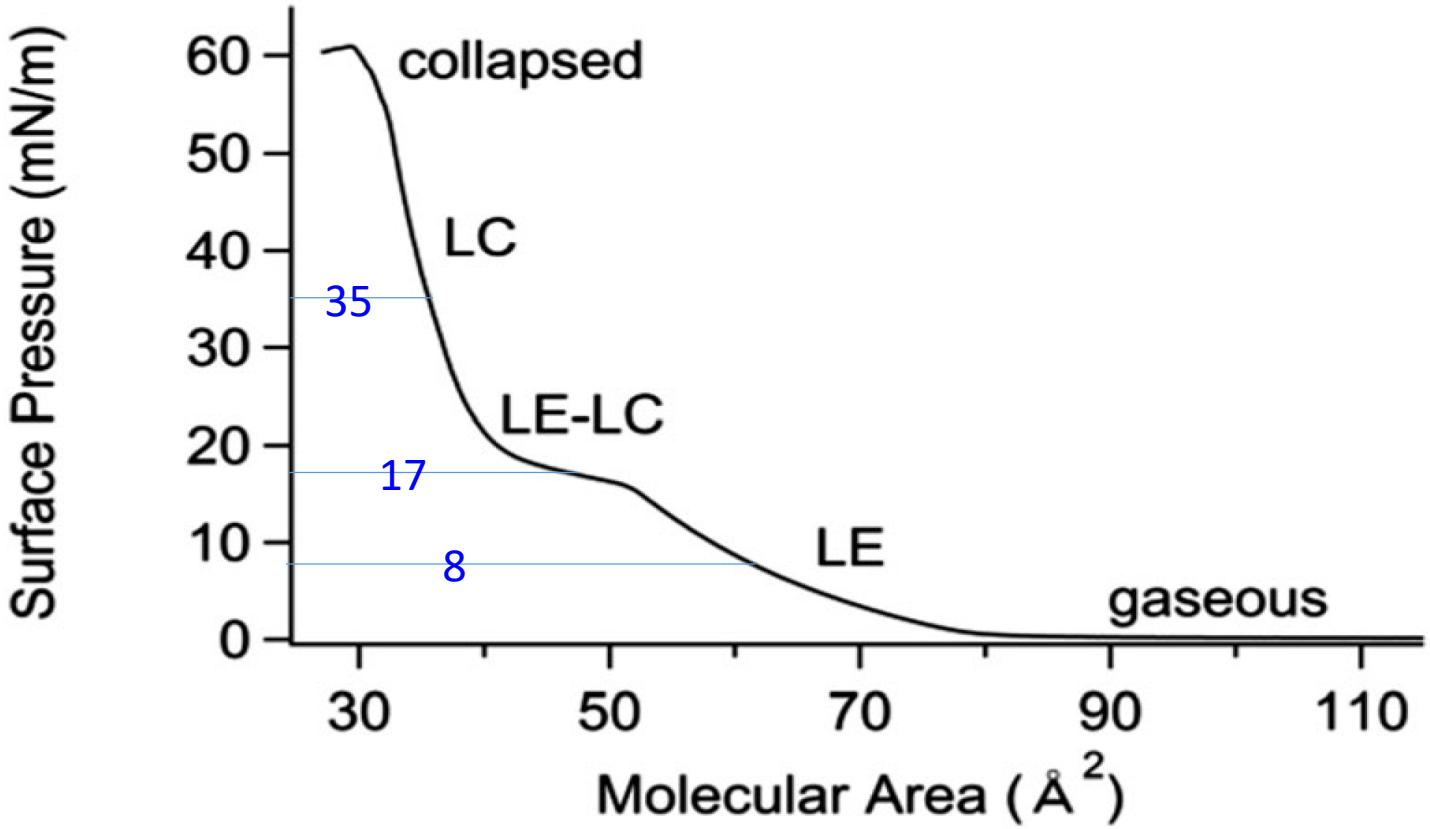

Fig. 5 π–A isotherm of d_{62}-DPPC on water at room temperature (25 °C).

Results and discussion [Im[$\chi^{(2)}$] spectra of d_{62}-DPPC Langmuir and LB monolayers]

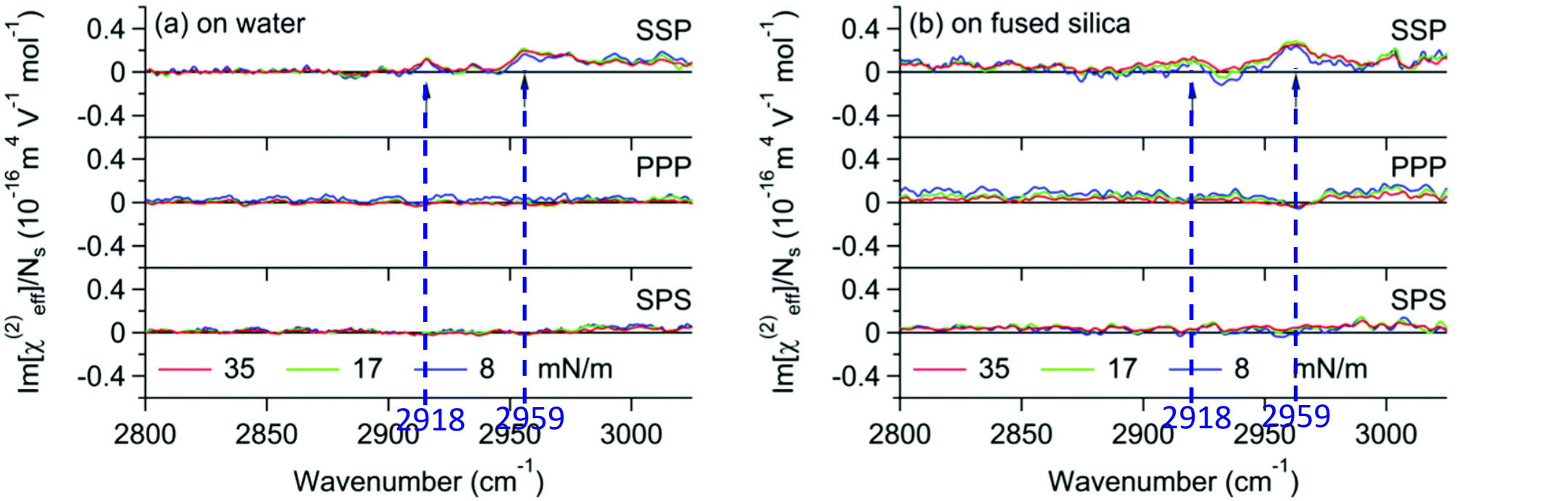

Fig. 6 Im[χ(2)] spectra of deuterated d_{62}-DPPC in the CH stretching region in the SSP, PPP, and SPS polarization combinations. (a) Langmuir monolayers on water and (b) LB monolayers on fused silica substrates. All spectra correspond to the susceptibility per one mole of lipid molecules. The arrows denote the vibrational bands attributed to the CH stretching modes in the head group of d62-DPPC.

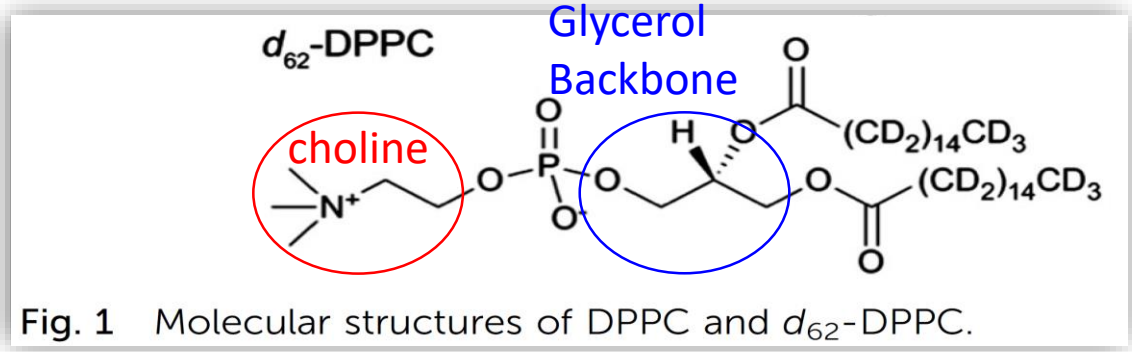

Fig. 1 Molecular structures of DPPC and d_{62}-DPPC.

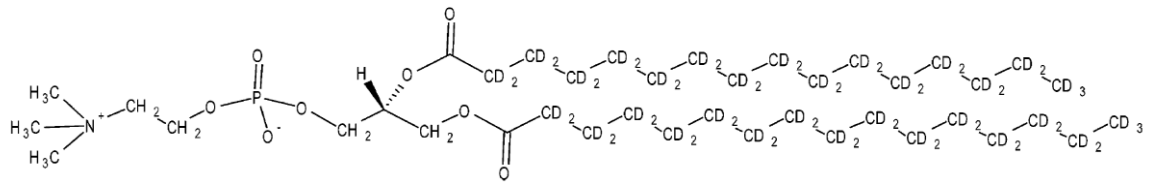

Results and discussion [Molecular conformations of DPPC monolayers]

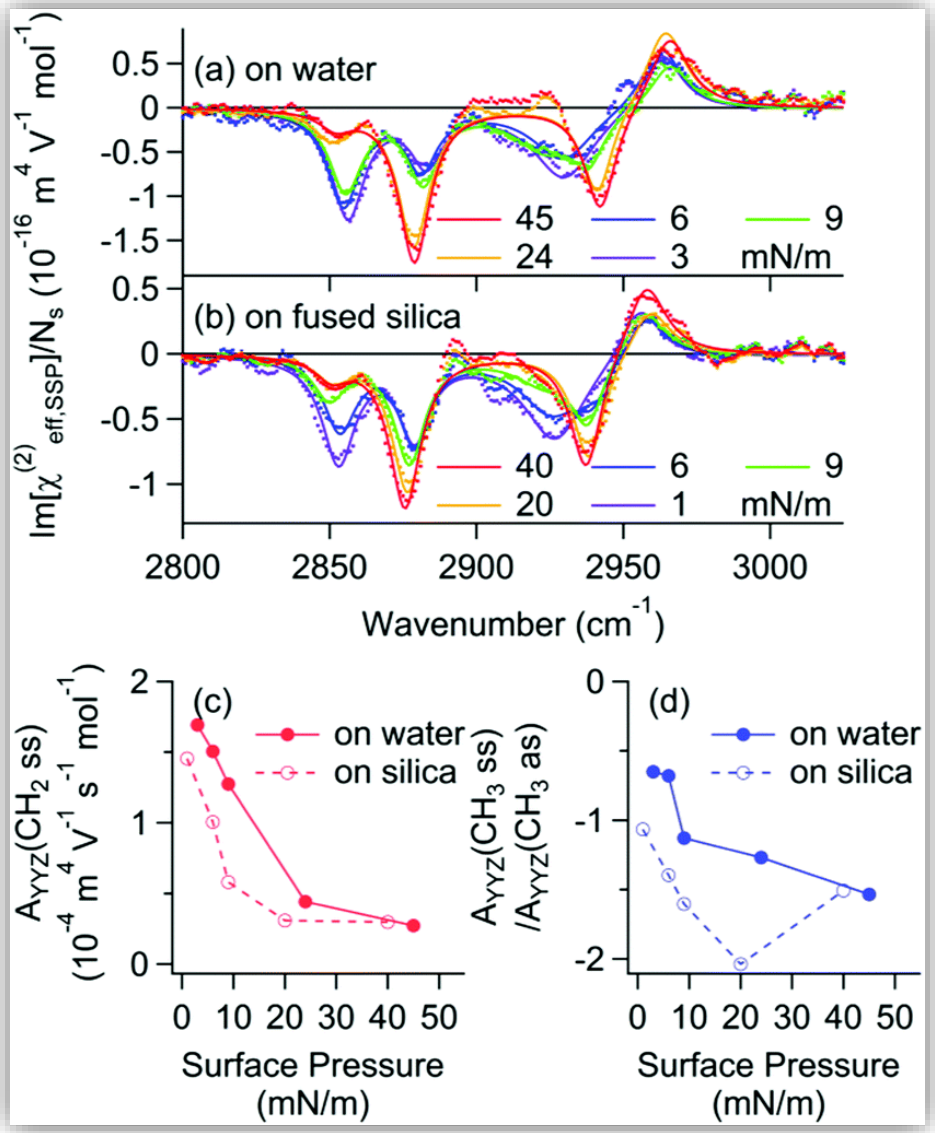

Fig. 7 Fitting results of Im[$\chi^{(2)}$] spectra of DPPC Langmuir monolayer on water (a) and LB monolayer on fused silica (b). In all observed spectra (dots), the corresponding Im[$\chi^{(2)}$] spectra of d_{62}-DPPC monolayer are already subtracted. Solid lines are spectral fits. Fresnel factor-corrected amplitude for CH_2 ss band (c) and the ratio of amplitudes for CH_3 ss and CH_3 as bands (d) as a function of surface pressure. In the fitting, both the imaginary and real parts of $\chi^{(2)}$ were simultaneously fitted.

- DPPC – d_{62}-DPPC give dots in (a) and (b)
- Solid lines are spectral fits.
- From fitting $A_{eff,q}$ can be obtained. q=qth vibrational resonance

$$\chi^{(2)}_{\mathrm{eff}} = \chi^{(2)}_{\mathrm{NR}} + \sum_q \frac{A_{\mathrm{eff},q}}{\omega_{\mathrm{IR}} - \omega_q + \mathrm{i}\Gamma_q}$$

$$\chi^{(2)}_{\mathrm{eff,SSP}} = L_{YY}(\omega_{\mathrm{SFG}})L_{YY}(\omega_{\mathrm{VIS}})L_{ZZ}(\omega_{\mathrm{IR}})\sin\theta_{\mathrm{IR}}\chi^{(2)}_{YYZ}$$

$$\frac{A_{\mathrm{eff,SSP},q}}{L_{YY}(\omega_{\mathrm{SFG}})L_{YY}(\omega_{\mathrm{VIS}})L_{ZZ}(\omega_{\mathrm{IR}})\sin\theta_{\mathrm{IR}}} = A_{YYZ,q}$$

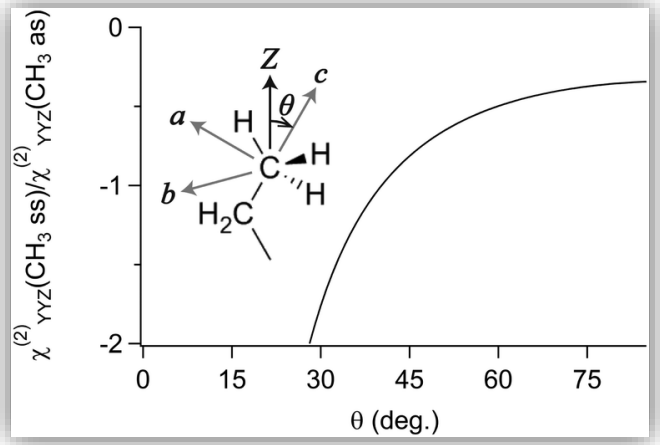

Fig. 8 Relationship between calculated $\chi^{(2)}_{YYZ}(CH_3\ ss)/\chi^{(2)}_{YYZ}(CH_3\ as)$ ratio and the tilt angle of the methyl group (θ).

- Number of gauche defects in DPPC molecule tends to decrease
- Average tilt angle of terminal methyl decreased

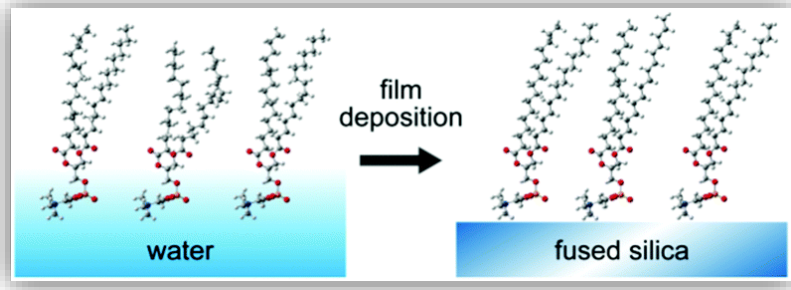

Fig. 9 Schematics of the structural change of DPPC monolayers due to the deposition from water to fused silica substrates.

Conclusion

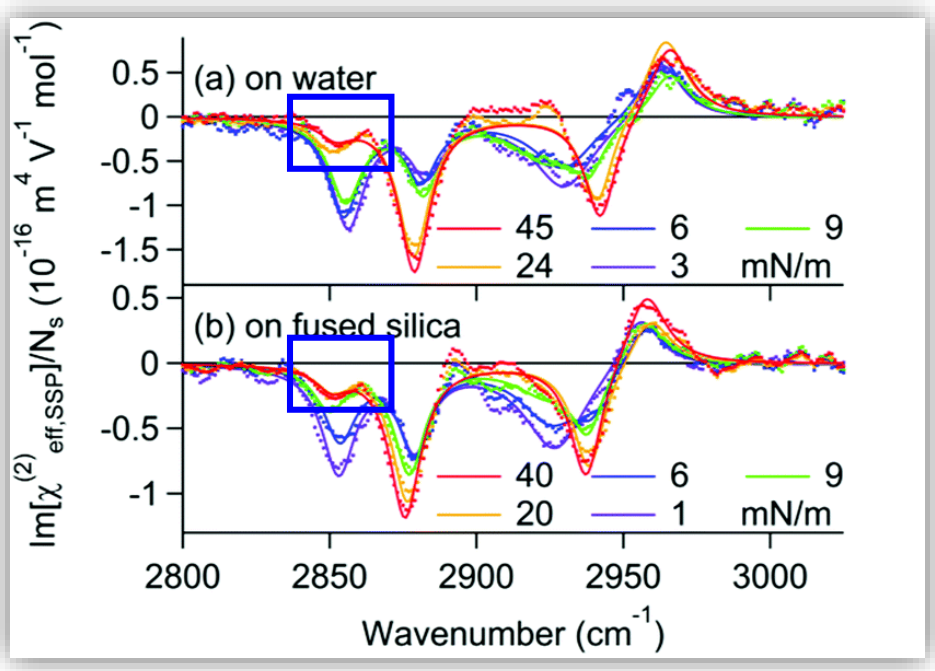

Still contain gauche defects even at relatively high surface pressure.

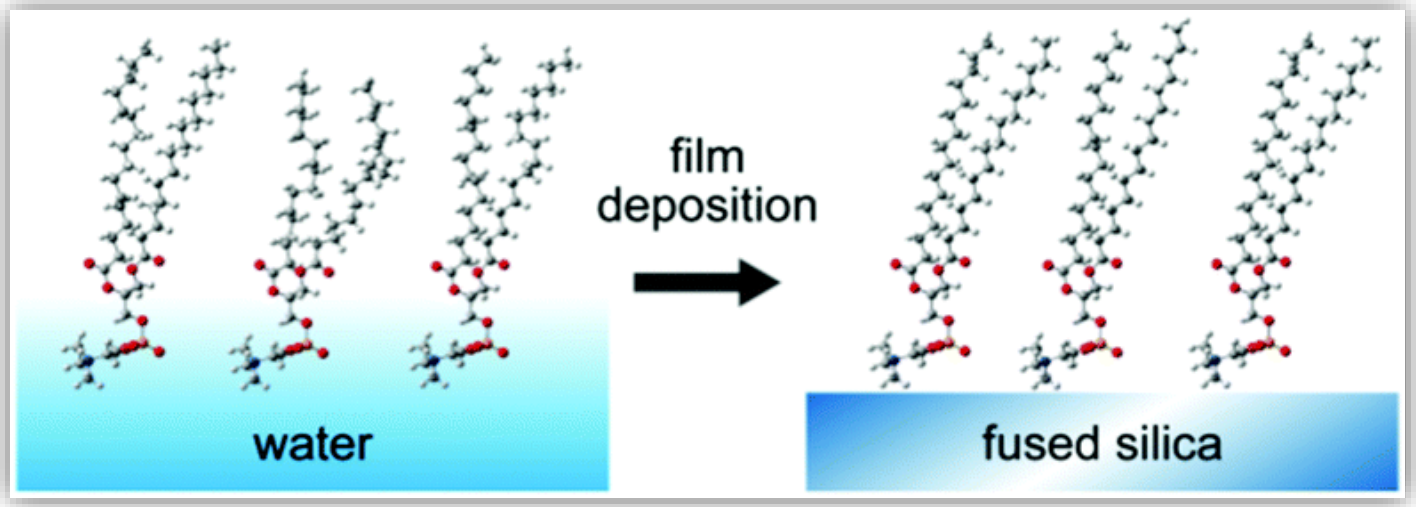

Film deposition onto solid substrates slightly decreases the number of gauche defects and decreases the tilt angle of terminal methyl groups.